

# Anisotropic pancake vortex transport in the crossing lattices regime of $\text{Bi}_2\text{Sr}_2\text{CaCu}_2\text{O}_{8+\delta}$ single crystals

M. Connolly,<sup>1</sup> S. J. Bending,<sup>1</sup> A. N. Grigorenko,<sup>2</sup> and T. Tamegai<sup>3</sup>

<sup>1</sup>*Department of Physics, University of Bath, Claverton Down, Bath, BA2 7AY, United Kingdom*

<sup>2</sup>*Department of Physics and Astronomy, University of Manchester, Manchester M13 9PL, United Kingdom*

<sup>3</sup>*Department of Applied Physics, The University of Tokyo, Hongo, Bunkyo-ku, Tokyo 113-8627, Japan*

(Received 7 July 2005; revised manuscript received 10 October 2005; published 7 December 2005)

We have used micro-Hall probe magnetometry to investigate how the out-of-plane “local” magnetization of a superconducting  $\text{Bi}_2\text{Sr}_2\text{CaCu}_2\text{O}_{8+\delta}$  single crystal depends on the strength and direction of an in-plane magnetic field,  $H_{\parallel}$ , in the crossing vortex lattices regime. The  $H_z=0$  remanent magnetization exhibits a pronounced anisotropy, being largest with  $H_{\parallel}$  parallel to the crystalline  $a$ -axis, and smallest when it is parallel to the orthogonal  $b$ -axis. We attribute this to the presence of strongly pinning linear defects (LDs), which are known to lie close to the  $a$ -axis in these crystals. With  $H_{\parallel}$  parallel to the  $a$ -axis Josephson vortex (JV) stacks become indirectly pinned along LDs, and channel pancake vortices (PVs) into these regions of high disorder, increasing the measured irreversibility. With  $H_{\parallel}$  along the  $b$ -axis PVs are efficiently channeled into the sample centre, readily cutting across LDs, and the irreversibility is low. At high temperatures the remanent magnetisation as a function of the in-plane field angle exhibits a pronounced shoulder which appears to be related to the critical accommodation angle for the indirect trapping of JVs by LDs, above which JVs snap free. At low temperatures random bulk pinning is increasingly in competition with LDs, and the measured anisotropy becomes much weaker.

DOI: [10.1103/PhysRevB.72.224504](https://doi.org/10.1103/PhysRevB.72.224504)

PACS number(s): 74.25.Qt, 74.25.Ha, 74.72.Hs

## I. INTRODUCTION

It is now accepted that very strong crystalline anisotropy in the high temperature superconductor  $\text{Bi}_2\text{Sr}_2\text{CaCu}_2\text{O}_{8+\delta}$  (BSCCO) leads to the formation of “crossing” vortex lattices for applied fields tilted more than a few degrees from the high symmetry  $c$ -axis.<sup>1,2</sup> In this regime, orthogonal sublattices of pancake vortex (PV) stacks and Josephson vortices (JVs) coexist. The former are directed along the crystalline  $c$ -axis and have their circulating supercurrents flowing within the  $\text{CuO}_2$  planes, while the latter lie in the  $a$ - $b$  plane, have “cores” which reside in the spaces between  $\text{CuO}_2$  planes, and highly anisotropic circulating currents derived partly from weak Josephson coupling between the planes. This anisotropic current distribution leads to strongly anisotropic JV-JV interactions and a rhombic vortex lattice whose unit cell is greatly stretched out in the  $a$ - $b$  plane. The JV supercurrents also induce a restructuring of PV stacks which leads to an attractive interaction between the crossing lattices,<sup>3</sup> as was clearly demonstrated in recent JV “decoration” experiments.<sup>4-7</sup> A further consequence of this interaction is that the penetration of pancake vortices under tilted magnetic fields becomes sensitive to the presence of JVs. Scanning Hall probe microscopy (SHPM) experiments<sup>4</sup> have revealed that the PV mobility along JV stacks is considerably higher than in JV-free regions, and the presence of JVs reduces the interaction between PVs and quenched “bulk” disorder, effectively depinning them. In addition, at fields just above the out-of-plane penetration field,  $H_p$ , PVs preferentially enter the sample along JVs, where the superposition of Meissner and JV currents at the edges leads to a slight lowering of Bean-Livingston penetration barriers,<sup>8</sup> and then enjoy a much higher mobility along the JV stacks.<sup>9,10</sup> Finally, it has

been demonstrated that stacks of JVs can become *indirectly* pinned via their interactions with strongly pinned pancake vortices.<sup>11</sup> Consequently, the irreversible out-of-plane magnetization under tilted magnetic fields is sensitive to the underlying JV structure and its relationship to the quenched disorder in the sample. We exploit this property in this work to explore the anisotropy of the disorder in an as-grown BSCCO single crystal.

BSCCO single crystals commonly exhibit correlated disorder which often takes the form of linear defects (LDs) aligned close to the  $a$ -axis growth direction<sup>12,13</sup> and strongly pins pancake vortices. The origin and composition of these defects is currently unclear. Evidence for their oxygen deficient stoichiometry, obtained by high resolution STEM-EDS,<sup>14</sup> is consistent with the enhanced pinning and preferential penetration of flux along the defects,<sup>15</sup> a behavior caused by the suppression of superconductivity and similar to that along weak intergranular links such as twin boundaries. Magneto-optical (MO) images of single crystals grown using the travelling solvent floating zone technique reveal that they extend along the entire length of the crystal with a nonuniform<sup>16</sup> spacing, suggesting that they could be small angle grain boundaries between individual crystallites.<sup>17,18</sup> However, recent observations of a second drop in the in-plane resistivity at  $T \sim 106$  K support the idea that they are needlelike intergrowths of the higher  $T_c$  Bi-2223 phase.<sup>19</sup> These linearly correlated defects pin high PV flux densities and have a striking indirect consequence on the local structure of the in-plane JV lattice. Due to the mutual attraction between the crossing lattices, a segment of a JV stack can be indirectly pinned along a LD by PVs directly pinned in the LD region. In addition, when the in-plane field subtends an angle  $\theta$  to the LDs, partially trapped JV stacks form kinks at

each defect-JV line intersection, analogous to the accommodation of tilted vortices by columnar defects<sup>20</sup> and twin boundaries.<sup>21</sup> SHPM images of this kinked structure have been analyzed by accounting for the anisotropy in an existing theory of vortex deformation by planar defects, to relate the length of the trapped segment,  $w$ , to  $\theta$ .<sup>11,22,23</sup> The elastic energy of the stretched JV string and the deformation of the surrounding JV “cage” is balanced against the additional crossing energy gained due to interaction with the extra pinned PV stacks on the LD. For angles smaller than a critical accommodation angle,  $\theta_{acc}$ ,  $w$  reduces with increasing angle according to

$$w \cos \theta = \sqrt{\frac{4\sigma}{K}} \left( \sqrt{\frac{\tan \theta_{acc} \sin \theta_{acc}}{\tan \theta \sin \theta}} - 1 \right), \quad (1)$$

where  $K = \Phi_0 B_{\parallel} / 4\pi\gamma\lambda^2$  arises from the “cage potential” interaction with neighboring Josephson vortices,  $\sigma \cong \Phi_0^2 / ((4\pi)^2 \gamma \lambda^2)$  is the JV line tension, and  $\theta_{acc}$  is defined by

$$\sin \theta_{acc} \tan \theta_{acc} = \frac{2U_p}{\sigma}, \quad (2)$$

where  $U_p$  is the *indirect* pinning potential per unit length. (Here  $\Phi_0$  is the flux quantum,  $B_{\parallel}$  is the in-plane induction,  $\gamma$  is the anisotropy parameter, and  $\lambda$  is the in-plane penetration depth.) For  $\theta \geq \theta_{acc}$ ,  $w=0$  and the Josephson vortex is straight and parallel to the in-plane field direction. In this paper we demonstrate that the out-of-plane “local” magnetization of a BSCCO crystal in a fixed applied in-plane field reflects this angle-dependent interaction between Josephson vortices and linear defects.

## II. EXPERIMENTAL METHOD

An as-grown BSCCO single crystal ( $T_c \sim 91$  K, dimensions  $\sim 2.5$  mm  $\times$  2 mm  $\times$  100  $\mu$ m) was fixed with low melting temperature paraffin wax to a low noise micro-Hall probe, patterned by electron beam lithography and wet etching in a GaAs/AlGaAs heterostructure two-dimensional electron gas, with an active flux sensing area of  $\sim 1$   $\mu$ m<sup>2</sup>. The Hall sensor was driven with a 10  $\mu$ A dc current from a precision source, and the measured Hall voltage amplified with a 10 000 $\times$  gain ultralow noise preamplifier, which incorporated electronic compensation of the  $H_z=0$  sensor offset. The magnetic field resolution of the entire measurement system at 85 K is  $\sim 1$  mG/ $\sqrt{\text{Hz}}$  or about  $10^{-4}\Phi_0/\sqrt{\text{Hz}}$ . The crystal was cleaved immediately prior to mounting and we estimate that the sample-sensor spacing is  $\sim 1$   $\mu$ m. The packaged sensor was mounted on the copper head of the sample insert for a temperature-controlled cryostat, and the crystallographic  $a$ - and  $b$ -axes of the crystal aligned to within  $\pm 10^\circ$  of the axes of two external Helmholtz coil pairs used to produce independent in-plane fields,  $H_{\parallel}^a$  and  $H_{\parallel}^b$ , up to  $\sim 36$  Oe. An out-of-plane field,  $H_z$ , was generated by a copper coil wound directly around the cryostat at the same height as the sample.

At the start of each measurement the sample was cooled in the Earth’s field to the desired temperature between 77 K

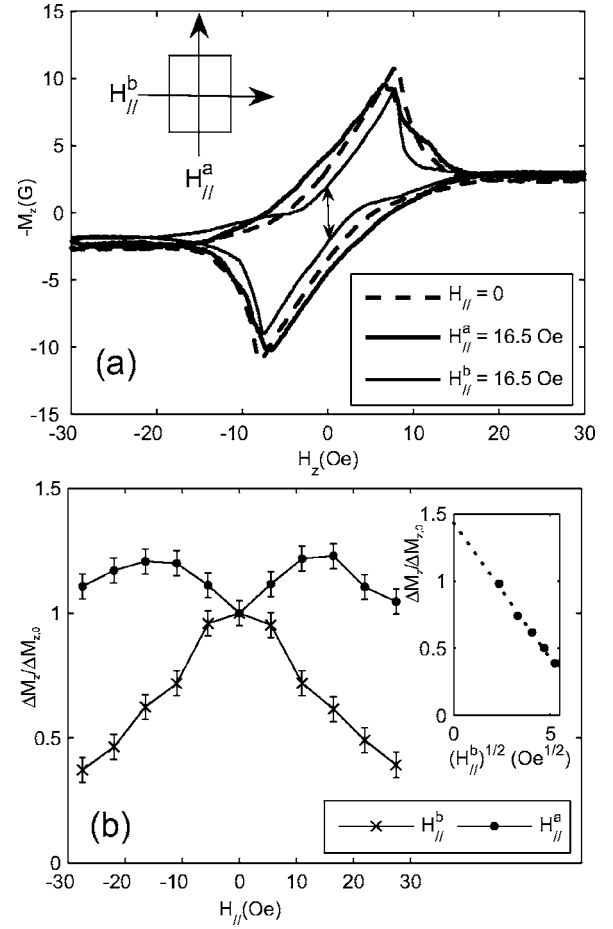


FIG. 1. (a) Plots of the “local” magnetization versus out-of-plane magnetic field at  $T=85$  K for  $H_{\parallel}=0$  (dashed line) and in-plane fields,  $H_{\parallel}^a=16.5$  Oe ( $H_{\parallel}^b=0$ ) and  $H_{\parallel}^b=16.5$  Oe ( $H_{\parallel}^a=0$ ) (solid lines, see inset). The vertical arrow indicates the zero-field remanence. (b) Normalized remanence,  $\Delta M_z / \Delta M_{z,0}$ , plotted against  $H_{\parallel}$  for the two in-plane field orientations, and (inset) against  $|H_{\parallel}^b|^{1/2}$  to illustrate the linear dependence of the JV channeling efficiency (dashed line is extrapolated from the linear fit to the high field data).

and  $T_c$ .  $H_{\parallel}^a$  and  $H_{\parallel}^b$  were then applied manually to generate the required field,  $H_{\parallel}$ , at an angle  $\theta$  to the  $a$ -axis. Finally the out-of-plane field,  $H_z$ , was swept around a measurement cycle between  $\pm 36$  Oe using a computer-controlled power supply, and the local magnetic induction at the Hall sensor,  $B_z$ , recorded at each point via an A/D converter. The first “virgin” trace was discarded, and the subsequent 25 cycles then averaged to improve the signal:noise ratio still further. The measured “local” out-of-plane magnetization ( $\mu_0 M_z = B_z - \mu_0 H_z$ ) was then constructed as a function of magnitude and angle of the in-plane field.

## III. RESULTS

Figure 1(a) illustrates typical out-of-plane local magnetization data at  $T=85$  K with no in-plane field ( $H_{\parallel}=0$ ) as well as  $H_{\parallel}=16.5$  Oe applied close to the  $a$ - or  $b$ -axes (see inset). Close inspection reveals that the zero-field irreversibility,  $\Delta M_z = M_z(H_z=0, dH_z/dt < 0) - M_z(H_z=0, dH_z/dt > 0)$ , de-

pends strongly on the magnitude and direction of the in-plane field. The data for  $a$ - and  $b$ -axis in-plane fields of varying magnitude are summarized in Fig. 1(b), where  $\Delta M_z$  has been normalized with respect to the value at  $H_{\parallel}=0$ ,  $\Delta M_{z,0}$ . We observe strikingly different behaviors for the two orthogonal directions. For fields applied close to the  $a$ -axis the irreversibility actually **increases** as  $H_{\parallel}$  is increased up to  $\sim 15$  Oe, beyond which it starts to fall again. In contrast, a reduction of the irreversibility is always observed as  $H_{\parallel}$  is increased parallel to the  $b$ -axis. The two different behaviors can almost certainly be related to the fact that the  $a$ -axis is parallel to the characteristic linear defects in these crystals, while the  $b$ -axis is perpendicular to them. The observation that the irreversibility falls monotonically for increasing in-plane fields directed along the  $b$ -axis is in line with previous reports.<sup>24</sup> It is consistent with the “channeling” of penetrating PVs along underlying JV stacks, which is known to suppress their interaction with quenched disorder and hence reduce the measured irreversibility.<sup>4,25</sup> The inset of Fig. 1(b) illustrates that, in fields greater than about 5 Oe, the decrease in the irreversibility in this geometry depends linearly on  $\sqrt{H_{\parallel}}$ . Since the lateral density of JV stacks,  $1/a_y = \sqrt{2}B_{\parallel}/\sqrt{3}\gamma\Phi_0$ , also depends on  $H_{\parallel}$  in the same way (the difference between  $H_{\parallel}$  and  $B_{\parallel}$  becomes small at fields above 5 Oe for our sample), this suggests that the reduction of irreversibility is simply proportional to the total number of JV stacks present in the sample in this regime. The fact that the fit line in the inset of Fig. 1(b) extrapolates to  $\sim 1.4$  at  $H_{\parallel}=0$ , instead of the expected value of 1, is not surprising. The effectively 1D process of PV motion along JVs will only suppress the irreversibility due to interactions with random and linear disorder when the JV stacks are sufficiently dense. At low fields, when the stack spacing is large, the measured changes in the irreversibility will be smaller than an estimate based on 1D effects alone. Another factor that contributes to this deviation is the difference between the applied field,  $H_{\parallel}$ , and the actual induction,  $B_{\parallel}$ , which yields the negative in-plane magnetization<sup>7</sup> due to JV screening currents, and is important at low fields.

The *increase* in the irreversibility when the in-plane field is parallel to the  $a$ -axis ( $H_{\parallel} < 15$  Oe) is a surprising result which has not been reported before. It does, however, have a natural explanation in terms of the indirect pinning of JV stacks interacting with strongly pinned PVs. For  $H_{\parallel}$  parallel to the  $a$ -axis, and hence the LDs, this would tend to trap JV stacks along linear defects. Therefore, at low in-plane fields the penetrating PVs are channelled into the regions of highest disorder, they become strongly pinned, and the irreversible magnetization increases. Within this scenario the maximum pinning occurs when there is quasicommensurability between the JV stacks and the disordered distribution of linear defects. At the peak field of  $H_{\parallel} \sim 15$  Oe the JV stack spacing in as-grown BSCCO ( $\gamma \sim 600$ ) is  $c_y \sim 20 \mu\text{m}$ , implying a similar mean lateral spacing between linear defects, in good agreement with estimates from both angular x-ray measurements<sup>13</sup> as well as the SHPM and MO images presented in Refs. 11 and 18 for crystals from the same source. As the in-plane field is increased above  $\sim 15$  Oe JV stacks increasingly start to fall *between* defect regions, which begin to channel penetrating PV stacks in the usual way, leading to

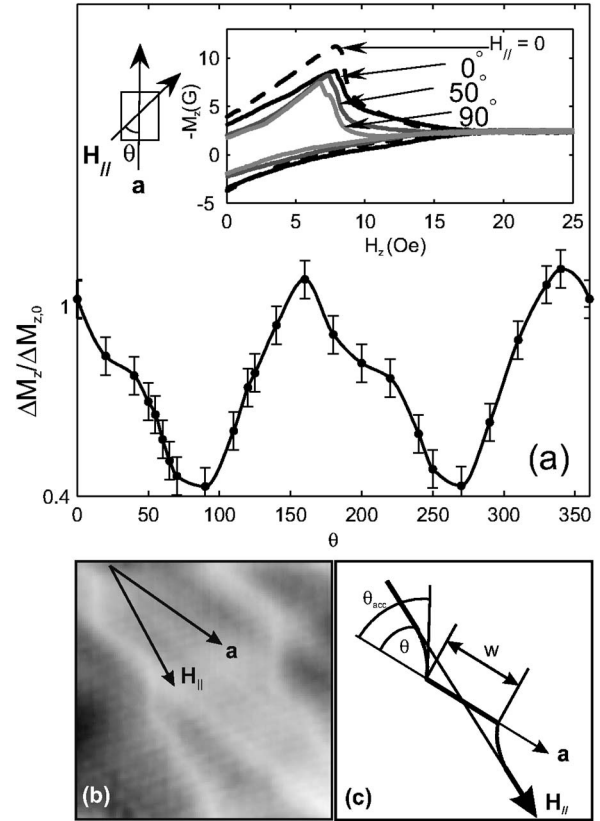


FIG. 2. (a) Normalized remanence,  $\Delta M_z/\Delta M_{z,0}$ , as a function of in-plane field angle (solid line is a guide to the eye). The right hand inset shows  $T=85$  K “local” magnetization loops for  $H_{\parallel}=0$  and  $H_{\parallel}=36$  Oe at different in-plane angles (see left hand inset for definition of  $\theta$ ). (b) SHPM image of kinked pancake vortex chains which are decorating underlying stacks of indirectly-pinned Josephson vortices at  $T=85$  K ( $H_z=10$  Oe,  $H_{\parallel}=34$  Oe, image size  $\sim 27.5 \times 27.5 \mu\text{m}^2$ ). (c) Sketch of the model used to describe vortex trapping.

a reduction in the irreversibility. The defect separations will be quite disordered in practice, but we expect the JV lattice to be able to deform to accommodate to this provided approximate commensurability is achieved. The relatively broad “matching peak” in Fig. 1(b) is consistent with this picture. We note that anisotropic pinning due to LDs was also observed in ac permeability measurements on BSCCO crystals with the ac excitation field parallel to the  $\text{CuO}_2$  planes. However, this work, presented in Ref. 13, focuses on the first order vortex melting transition, and was not interpreted in terms of crossing lattices.

Figure 2(a) illustrates how the normalised irreversibility,  $\Delta M_z/\Delta M_{z,0}$ , varies as a function of in-plane field angle,  $\theta$ , for a fixed in plane field strength,  $H_{\parallel}=36$  Oe. In this experiment, the two pairs of Helmholtz coils were driven by two separate power supplies to give the required in-plane field vector. We find that  $\Delta M_z(\theta)$  displays a  $180^\circ$  rotation symmetry as expected from the rectangular symmetry of the BSCCO crystal, but pronounced shoulders around  $55^\circ$  and  $235^\circ$  break the expected  $\Delta M_z(\theta) = \Delta M_z(-\theta)$  symmetry. These angles are close to the accommodation angle beyond which a JV is unable to become even partially indirectly pinned along

a linear defect. JV trapping has been clearly observed in earlier SHPM measurements<sup>11</sup> in very similar crystals to the one studied here. Figure 2(b) shows a typical image which contains two partially pinned JV stacks in a sample at  $T=85$  K where an in-plane field of 34 Oe has been applied at an angle of about  $30^\circ$  to the  $a$ -axis. It can be shown that the accommodation angle defined in Eq. (2) can be identified with the angle at which elastic JV strings approach the linear defect parallel to the  $a$ -axis [cf. sketch in Fig. 2(c)]. Hence we can estimate that  $\theta_{\text{acc}} \sim 65^\circ$  for this image. Beyond the accommodation angle the length of the trapped JV segment drops to zero and the channeling of penetrating PVs should be greatly enhanced, since they are no longer being forced to travel along the linear defects in the indirectly pinned regions. The angular shift of  $\sim -10^\circ$  of the shoulder positions from the expected accommodation angles must be partly due to a slight misalignment of the BSCCO crystal relative to the Helmholtz coils. However, within vortex trapping theory it is the LD direction which defines the angular origin, and MO images<sup>18</sup> suggest that it can deviate by up to  $\sim 10^\circ$  from the  $a$ -axis.

The broken  $\Delta M_z(\theta) = \Delta M_z(-\theta)$  symmetry must stem from some irreversibility associated with the vortex trapping that depends on the measurement history. The in-plane fields in Fig. 2(a) were rotated monotonically in a positive sense from  $\theta=0^\circ$ , and the broken symmetry must arise from the details of the trapping of elastic Josephson vortex strings under these conditions. For example, at small angles ( $\theta \sim 0^\circ$ ) the JVs will be readily trapped on linear defects since they run almost parallel to them. Furthermore, even when the out-of-plane field is reduced to zero, enough strongly pinned PVs remain in the sample to ensure the indirect pinning of JVs. Hence, when the in-plane field is rotated to a new angle the JV system retains a memory of its history. Once the angle exceeds the accommodation angle the JVs snap away from the linear defects and become straight. If one continues rotating the JV system beyond the second accommodation angle [ $\theta > (180^\circ - \theta_{\text{acc}})$ ] there will be a large barrier for the straight JV strings to deform and find their equilibrium trapping state. Hence it is likely that metastable straight JVs are found even well within the accommodation angle (and also metastable trapped JVs outside the accommodation angle) giving rise to the observed asymmetry as  $\theta_{\text{acc}}$  is approached from above or below. This picture has been confirmed by varying the in-plane field angle in both a positive and negative sense at  $T=77$  K. For the former situation a shoulder was observed at  $\theta \sim 55^\circ$  in agreement with Fig. 2(a), while for the latter it only formed at the second accommodation angle  $\theta \sim -75^\circ$  ( $\equiv +285^\circ$ ).

Figure 3 illustrates how the normalised irreversibility in the range  $0^\circ \leq \theta \leq 90^\circ$  changes with temperature. At lower temperatures, due to a reduction in PV thermal energy, bulk pinning of PVs dominates over PV trapping and channeling along JVs, and we observe an overall increase in the number of PV stacks pinned at  $H_z=0$ . [The ratio of PV bulk pinning energy to crossing energy of PV-JV interaction is proportional to  $1/\lambda(T)^2$  and hence is higher at low temperatures.<sup>3</sup>] In this regime the influence of channeling is therefore reduced, and the irreversibility is a relatively weak function of

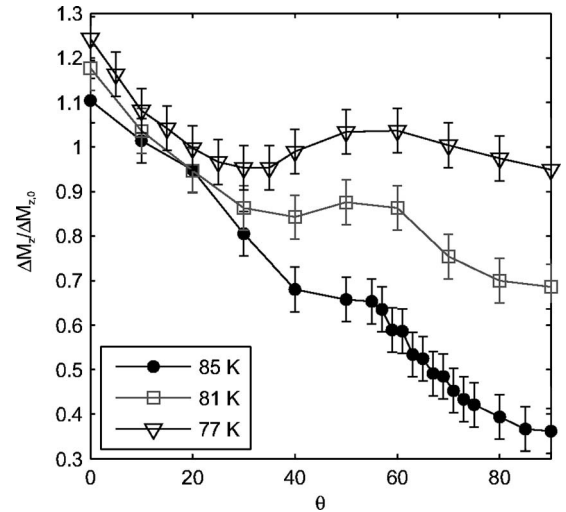


FIG. 3. Temperature dependence of the normalized remanence,  $\Delta M_z/\Delta M_{z,0}$ , as a function of  $H_{\parallel}$  direction in the vicinity of the trapping shoulder around the accommodation angle.

angle. It is interesting to note that even in the absence of efficient channeling, the JV-PV interaction with LDs still produces a weak peak around the accommodation angle. We speculate that this is due to increased meandering of JV stacks in this angular range arising from indirect pinning on strong pointlike pinning sites in addition to linear defects. In contrast, at high temperatures ( $T=85$  K) the system appears to be dominated by channeling on JVs, the shoulder near  $55^\circ$  is very pronounced, and the irreversibility drops by almost a factor of four on rotating the in-plane field from the  $a$ - to  $b$ -axis.

#### IV. CONCLUSIONS

In conclusion we have used a micro-Hall probe to investigate how the local  $c$ -axis magnetization of a BSCCO single crystal is influenced by the strength and direction of an in-plane field. With the in-plane field along the crystalline  $b$ -axis the irreversibility falls linearly as  $\sqrt{H_{\parallel}}$ , suggesting that it is simply proportional to the lateral JV stack density. In contrast we observe an increase in the out-of-plane irreversible magnetization as the in-plane field is increased along the  $a$ -axis up to  $\sim 15$  Oe. This result is surprising, since the presence of JVs is usually assumed to suppress the irreversible magnetization, and is explained within the crossing lattices picture by considering the dynamics of PVs along JVs which are indirectly pinned on linear defects. The maximum in irreversibility near  $H_{\parallel}=15$  Oe suggests that the JV stack spacing is quasicommensurate with the mean lateral spacing of linear defects at this field, leading to an estimate for the average LD spacing of  $\sim 20 \mu\text{m}$ , in good agreement with other measurements. When  $\theta$  is increased in a positive sense we find that the irreversibility exhibits distinct shoulders around  $55^\circ$  and  $235^\circ$  which, in combination with SHPM images of the vortex structure under similar experimental conditions, leads us to conclude that these angles are connected to the critical accommodation angle predicted by vortex trap-

ping theory. The out-of-plane magnetisation depends on the history of the prepared in-plane field state, indicating that there is irreversibility associated with the trapping process which makes it depend on the sense of rotation. The suppression of the irreversibility is a fairly weak function of angle at low temperatures, when the interaction between the crossing sublattices is weak in comparison to bulk PV pinning forces, but can lead to a reduction of  $\Delta M_z$  by a factor of 4 at high temperatures when the system is dominated by channeling along JVs. We conclude that the out-of-plane irreversibility

of BSCCO single crystals is a sensitive measure of correlated anisotropic disorder over a wide range of temperatures in the crossing lattices regime.

#### ACKNOWLEDGMENTS

This work was supported by an EPSRC-funded Ph.D. studentship in the UK and a Grant-in-aid for Scientific Research from the Ministry of Education, Culture, Sports, Science, and Technology, Japan.

- 
- <sup>1</sup>L. N. Bulaevskii, M. Ledvij, and V. G. Kogan, *Phys. Rev. B* **46**, 366 (1992).  
<sup>2</sup>D. A. Huse, *Phys. Rev. B* **46**, 8621 (1992).  
<sup>3</sup>A. E. Koshelev, *Phys. Rev. Lett.* **83**, 187 (1999).  
<sup>4</sup>A. Grigorenko, S. J. Bending, T. Tamegai, S. Ooi, and M. Henini, *Nature (London)* **414**, 728 (2001).  
<sup>5</sup>V. K. Vlasko-Vlasov, A. Koshelev, U. Welp, G. W. Crabtree, and K. Kadowaki, *Phys. Rev. B* **66**, 014523 (2002).  
<sup>6</sup>M. Tokunaga, M. Kobayashi, Y. Tokunaga, and T. Tamegai, *Phys. Rev. B* **66**, 060507(R) (2002).  
<sup>7</sup>A. N. Grigorenko, S. J. Bending, I. V. Grigorieva, A. E. Koshelev, T. Tamegai, and S. Ooi, *Phys. Rev. Lett.* **94**, 067001 (2005).  
<sup>8</sup>L. Burlachkov, V. B. Geshkenbein, A. E. Koshelev, A. I. Larkin, and V. M. Vinokur, *Phys. Rev. B* **50**, R16770 (1994).  
<sup>9</sup>M. Tokunaga, T. Tamegai, Y. Fasano, and F. de la Cruz, *Phys. Rev. B* **67**, 134501 (2003).  
<sup>10</sup>S. J. Bending, A. N. Grigorenko, I. A. Crisan, D. Cole, A. E. Koshelev, J. R. Clem, T. Tamegai, and S. Ooi, *Physica C* **412–414**, 372 (2004).  
<sup>11</sup>A. N. Grigorenko, S. J. Bending, A. E. Koshelev, J. R. Clem, T. Tamegai, and S. Ooi, *Phys. Rev. Lett.* **89**, 217003 (2002).  
<sup>12</sup>M. V. Indenbom, C. J. van der Beek, V. Berseth, T. Wolf, H. Berger, and W. Benoit, *J. Low Temp. Phys.* **105**, 1529 (1996).  
<sup>13</sup>J. A. Herbsommer, V. F. Correa, G. Nieva, H. Pastoriza, and J. Luzuriaga, *Solid State Commun.* **120**, 59 (2001).  
<sup>14</sup>I-Fei Tsu, Jyh-Lih Wang, S. E. Babcock, A. A. Polyanskii, D. C. Larbalestier, and K. E. Sickafus., *Physica C* **349**, 8 (2001).  
<sup>15</sup>G. Yang, J. S. Abell, and C. E. Gough, *Physica C* **341–348**, 1091 (2000).  
<sup>16</sup>Yanina Fasano, M. Menghini, F. de la Cruz, and G. Nieva, *Phys. Rev. B* **62**, 15183 (2000).  
<sup>17</sup>M. R. Koblischka, R. J. Wijngaarden, D. G. de Groot, R. Griesen, A. A. Menovsky, and T. W. Li, *Physica C* **249**, 339 (1995).  
<sup>18</sup>M. Yasugaki, M. Tokunaga, N. Kameda, and T. Tamegai, *Phys. Rev. B* **67**, 104504 (2003).  
<sup>19</sup>M. Li, P. H. Kes, S. F. W. R. Rycroft, C. J. van der Beek, and M. Konczykowski, *Physica C* **408–410**, 25 (2004).  
<sup>20</sup>V. Hardy, A. Wahl, S. Hebert, A. Ruyter, J. Provost, D. Groult, and Ch. Simon, *Phys. Rev. B* **54**, 656 (1996).  
<sup>21</sup>G. Blatter, J. Rhyner, and V. M. Vinokur, *Phys. Rev. B* **43**, 7826 (1991).  
<sup>22</sup>L. M. Paulius, J. A. Fendrich, W. K. Kwok, A. E. Koshelev, V. M. Vinokur, G. W. Crabtree, and B. G. Glagola, *Phys. Rev. B* **56**, 913 (1997).  
<sup>23</sup>A. E. Koshelev (unpublished).  
<sup>24</sup>D. E. Farrell, E. Johnston-Halperin, L. Klein, P. Fournier, A. Kapitulnik, E. M. Forgan, A. I. M. Rae, T. W. Li, M. L. Trawick, R. Sasik, and J. C. Garland, *Phys. Rev. B* **53**, 11807 (1996).  
<sup>25</sup>M. Yasugaki, K. Itaka, M. Tokunaga, N. Kameda, and T. Tamegai, *Phys. Rev. B* **65**, 212502 (2002).